17th Brazilian Congress of Thermal Sciences and Engineering
November 25th-28th, 2018, Águas de Lindóia, SP, Brazil

ENCIT-2018-0412
EXPANSION NOISE IN HOUSEHOLD REFRIGERATORS: AN EXPERIMENTAL STUDY

Carlos Boabaid Neto
Federal Institute of Santa Catarina - José Lino Kretzer 609, 88103-310, São José, SC, Brazil
boabaid@ifsc.edu.br

Cláudio Melo
POLO Research Laboratories for Emerging Technologies in Cooling and Thermophysics - Federal University of Santa Catarina, 88040-900, Trindade, Florianópolis, SC, Brazil
melo@polo.ufsc.br

Arcanjo Lenzi
André L. G. Caetano
Acoustics and Vibration Laboratory - Federal University of Santa Catarina, 88040-900, Trindade, Florianópolis, SC, Brazil
arcanjo.lenzi@ufsc.br
caetano@lva.ufsc.br

Abstract. *Among the sources of noise in refrigerators, the expansion noise produced by the flow through the expansion device is one of the least understood. The aim of this study was to investigate experimentally the acoustic excitation generated by the expansion process in a typical household refrigerator equipped with capillary tube, employing direct measurement of the acoustic pressure within the refrigerant flow. A transparent filter-dryer was used in order to visualize the flow pattern at the capillary tube inlet. Tests were carried out under several operating conditions. It was observed that a vortex is formed at the capillary tube inlet under certain conditions. The jet flow at the capillary tube outlet was the dominant source of acoustic excitation associated to the expansion process. A larger diameter capillary tube produced lower levels of acoustic excitation, especially when combined with a higher refrigerant charge. Reducing the speed of the compressor had the effect of reducing the acoustic excitation. The initial period of the operating cycle of the system was the most critical. The acoustic excitation was higher in after-defrost cycles. For the condition of continuous vortex formation, the acoustic excitation showed the lowest levels. The findings bring valuable information to the design of household refrigerators.*

Keywords: *refrigerator, capillary tube, expansion noise*

1. INTRODUCTION

Noise generated by household refrigerators is an important subject. Because they are installed predominantly in residential environments, which often provide good acoustic propagation conditions (Jeon *et al.*, 2007), and as they remain in operation uninterruptedly, their acoustic emission deserves attention because high noise levels or anomalous noises annoy the user, increasing the costs associated with service calls and adversely affecting how consumers perceive the product and the manufacturer.

The noise radiated by a refrigerator is generated by the vibration of the surfaces in direct contact with the surrounding air. There are two main excitation sources in a refrigerator: (i) vibrating components (compressor and fan); and (ii) fluid flow (airflow inside the cabinet and refrigerant flow). The refrigerant flow generates acoustic excitations (fluctuations of pressure and density; Reethof, 1978), which generate forces acting on the inner surface of the pipes, transmitting energy that manifests itself as structural vibrations, and this vibratory energy propagates through the solid structures. The cabinet and other surfaces then radiates this energy as airborne noise (Caetano, 2013). Thus, any noise associated to the refrigerant flow results from the coupling between two distinct sets of phenomena: the fluid-acoustic (the generation and propagation of the acoustic excitation internally to the flow) and the vibro-acoustic (the propagation and transmission of vibratory excitation through the structures).

The expansion process is an important source of acoustic excitation (Singh *et al.*, 1999). Due to the intrinsic characteristics of the expansion process a turbulent, two-phase compressible flow is generated that can reach the critical condition (Wallis, 1980). At the expansion device outlet a jet is formed and this flow configuration can lead to intense acoustic excitation (Lighthill, 1963; Reethof, 1978; Tam, 1995).

In household refrigerators, the capillary tube is the most common expansion device and, in most cases, the configuration where the suction line is placed in physical contact with the capillary tube (named the capillary tube-

suction line heat exchanger) is employed. This configuration allows for the flow within the capillary tube to be cooled by the refrigerant vapor flowing along the suction line, resulting in an increase of refrigerating capacity and higher COP. The flow along the capillary tube exhibits several complex phenomena: the vaporization of the refrigerant fluid generates discontinuous non-homogeneous two-phase flow patterns (Tannert and Hesse, 2016; Apaydin and Heperkan, 2016); metastable flow can occur (Chen, 1997); and the cooling of the vapor bubbles within the capillary tube flow along the heat exchanger can be a source of anomalous noise (McLevige and Miller, 2001; Hartmann and Melo, 2013).

The aim of this study was to achieve a better understanding of the phenomena involved in the generation of acoustic excitation by the expansion process in a refrigerator equipped with the capillary tube-suction line heat exchanger.

2. EXPERIMENTAL METHODS

A review of the relevant literature as well as the investigations performed by the authors revealed that the noise associated with the expansion process in a refrigerator is of a complex, non-stationary nature. Furthermore, traditional analysis based on the measurement of the noise emitted by the refrigerator, including the anomalous noises sometimes reported, and its subjective qualification according to its resemblance to other common sounds (whistling, scratching, etc.) may result inaccurate and misleading, since the same source can yield sounds of different characteristics, depending on the materials and constructive characteristics of each individual refrigerator, and these differences can be erroneously attributed to different sources. This inaccuracy arises from the fact that the usual approach does not allow to distinguish between the fluid-acoustic and the vibro-acoustic phenomena. With the aim of avoiding this confusion and reducing this inaccuracy, the direct measurement of the acoustic excitation within the refrigerant fluid flow was performed in this study. With the simultaneous measurement of the thermodynamic conditions of the flow, the relationship between the flow phenomena and the acoustic phenomena could be examined.

The experimental work was carried out on a typical frost-free, bottom-mount refrigerator, equipped with a variable-speed reciprocating compressor, fin-and-tube evaporator and a concentric capillary tube-suction line heat exchanger, running with R600a refrigerant. T-type thermocouples were employed to measure the temperature and foil strain-gage transducers to measure the absolute pressure. Acoustic pressure measurements were carried out with diaphragm piezoelectric sensors, with a sensitivity of 14.5 mV kPa^{-1} and resolution of 7 Pa. Acceleration measurements were carried out with piezoelectric accelerometers (6.2 mm OD, 1.5 g mass) with a sensitivity of 10 mV g^{-1}. Details on the refrigeration loop and instrumentation lay-out are given in Boabaid Neto *et al.*, (2014).

The acoustic pressure sensors were installed by using an appropriate housing (Boabaid Neto *et al.*, 2014), in a manner that it was able to detect the pressure fluctuations inner to the tubes. Figure 1 shows the lay-out of the acoustic pressure sensor mounting after the capillary tube outlet, evidencing how this sensor is able to capture the acoustic excitation generated by the jet flow formed at the capillary tube outlet.

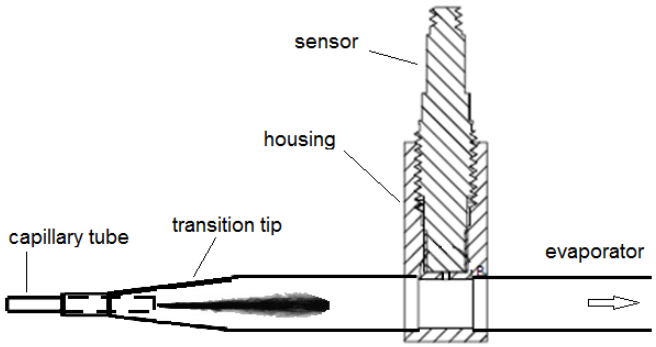

Figure 1. Lay-out of the acoustic pressure sensor mounting after the capillary tube outlet.

In refrigerators, the capillary tube is in general directly attached to the filter-dryer. A transparent filter-dryer was employed to allow for the visualization of the flow conditions at the capillary tube inlet (Fig. 2 and 3). The flow was continuously monitored with a webcam-type camera.

Tests were conducted in a room with low background noise levels. Due to the effect of the ambient temperature on the refrigerating system, a specially adapted air-conditioning system was installed, which was capable of maintaining the room temperature at the desired levels, within a range of ±0.3°C during the tests.

Two data acquisition systems were used, one (DAQ 1) for the measurement of the thermodynamic variables (temperature, absolute pressure, compressor speed) and the other (DAQ 2) for the measurement of acoustic variables (acoustic pressure, acceleration and ambient noise). All of the physical parameters as well as the images of the filter-dryer were recorded during a complete operating cycle on a PC, which was also used to control the acquisition systems and store the data. Due to the characteristics of the acquisition system and the amount of the instrumentation installed, thermodynamic data were registered by DAQ 1 every 7 to 8 s. DAQ 2 registered the frequency spectrum and the global

level (*rms* value for the instantaneous fluctuations) of the signal of each acoustic sensor every 0.78 s. Due to the distinct recording frequency of each data group, statistical methods were employed to allow a comparison between the thermodynamic and acoustic variables and identify correlations between them. Thus, averages of all measurements were taken from samples of the signals extracted at 2-min intervals during the period of greatest stabilization along the operating cycle of the refrigeration system. The signal picked up by the accelerometer installed at the evaporator inlet was converted into an audible signal by the sonification technique (McGee, 2009), enabling a qualitative sound evaluation of the signal.

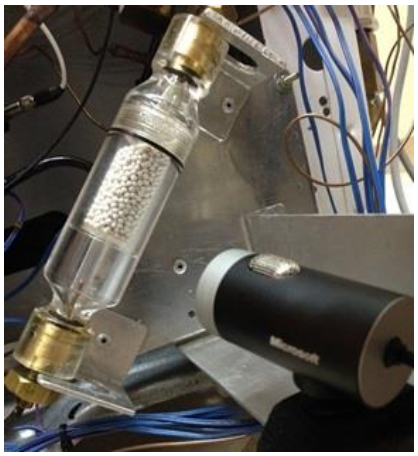

Figure 2. Transparent filter-dryer and monitoring camera.

Figure 3. Flow monitoring at the filter-dryer, under typical conditions.

Table 1 summarizes the expanded measurement uncertainty (U) for the main measured parameters. The standard uncertainty was calculated through a combination of Type A and Type B methods (JCGM, 2008), and the expanded uncertainty was defined with a confidence interval of 95.45% probability.

Table 1. Typical expanded uncertainty associated with the measured parameters.

Parameter	Unit	U ±
Temperature	°C	0.24
Absolute pressure, high	bar	0.035
Absolute pressure, low	bar	0.020
Acoustic pressure	Pa	3.9
Acceleration	m s^{-2}	0.023

2.1 Experimental design

Due to the complexity of the phenomena, and with the aim of identifying the most relevant effects with a reduced amount of tests, the factorial design technique (Box *et al.*, 2005) was employed. The following factors (independent variables) were selected: /i/ inner diameter of the capillary tube; /ii/ refrigerant charge; /iii/ rotational speed of the compressor; and /iv/ ambient temperature.

The inner diameter of the capillary tube is the main factor affecting the performance of the system and, for this reason, this parameter was tested at 3 levels. The other factors were tested at 2 levels, resulting in a 3 x 2^3 design, as shown in Table 2, where 'ID' indicates de inner diameter of the capillary tube, 'rc' is the refrigerant charge, 'T_{amb}' is the room temperature, and 'Speed' denotes the compressor rotational speed. The inner diameter of the capillary tubes was measured according to the ASHRAE Standard 28-1996 method (ASHRAE, 1996), with expanded uncertainty values of ±0.022 mm, ±0.008 mm and ±0.013 mm for the smaller, the intermediate and the bigger diameter respectively. The length of the capillary tubes (about 3 m) and the length and relative position of the suction line heat exchangers were the same for all configurations. Although the change of the inner diameter of the capillary tube substantially changes the refrigerant flow and consequently the stabilized operating point of the refrigeration system, which would require the adjustment of its length, the length was kept constant precisely in order to provide a broader range of flow and thermodynamic conditions.

The original refrigerant charge of the system was 56 g, which was established as the low level. An additional charge of 15 g was defined as the high level. The high level for the rotational speed of the compressor is an average value for

fixed-speed compressors operating on an AC 60 Hz electrical grid, and the low level is a typical value for variable-speed compressors under partial-load conditions. Levels for the ambient temperature were restricted by the control range of the ambient control system of the test room. Other conditions, presented in Table 3, were also tested in order to observe particular trends in the behavior of the dependent variables.

Table 2. Factors and levels of the factorial analysis

Test	ID [mm]	rc [g]	T_{amb} [°C]	Speed [rpm]	Test	ID [mm]	rc [g]	T_{amb} [°C]	Speed [rpm]	Test	ID [mm]	rc [g]	T_{amb} [°C]	Speed [rpm]
1	0.643	56	20	1600	9	0.767	56	20	1600	17	0.520	56	20	1600
2	0.643	56	20	3500	10	0.767	56	20	3500	18	0.520	56	20	3500
3	0.643	56	25	1600	11	0.767	56	25	1600	19	0.520	56	25	1600
4	0.643	56	25	3500	12	0.767	56	25	3500	20	0.520	56	25	3500
5	0.643	71	20	1600	13	0.767	71	20	1600	21	0.520	71	20	1600
6	0.643	71	20	3500	14	0.767	71	20	3500	22	0.520	71	20	3500
7	0.643	71	25	1600	15	0.767	71	25	1600	23	0.520	71	25	1600
8	0.643	71	25	3500	16	0.767	71	25	3500	24	0.520	71	25	3500

Table 3. Levels for additional tests

Test	ID [mm]	rc [g]	T_{amb} [°C]	Speed [rpm]	Test	ID [mm]	rc [g]	T_{amb} [°C]	Speed [rpm]	Test	ID [mm]	rc [g]	T_{amb} [°C]	Speed [rpm]
25	0.767	56	20	4000	30	0.520	56	20	4000	35	0.520	41	20	3500
26	0.767	56	25	2500	31	0.520	56	25	4000	36	0.520	41	25	1600
27	0.767	56	25	4000	32	0.520	71	20	4000	37	0.520	41	25	3500
28	0.767	71	20	2500	33	0.520	71	25	4000					
29	0.767	71	25	2500	34	0.520	41	20	1600					

In frost-free refrigerators, the frost formed on the surface of the evaporator must be removed periodically. During a defrost operation, the evaporator is intensely heated by the use of an encapsulated resistive electric heater mounted directly on the evaporator. Thus, when the subsequent operating cycle is triggered, the performance of the cooling system are quite different from those of a normal operating cycle. To evaluate the impact of this situation on the acoustic variables, the operating cycle immediately after a defrost operation was also recorded, for the operating conditions of Tests 9-37. Thus, the experimental study totalized 66 tests.

3. RESULTS

3.1 Characterization of the flow at filter-dryer (capillary tube inlet)

Due to its larger inner diameter, flow speeds inside the filter-dryer are very low, and phase separation can occur, establishing a well-defined liquid-vapor interface (Fig. 4). This configuration allows the formation of a vortex (Möller *et al.*, 2012), that is capable of entrain vapor into the capillary tube.

In the refrigerator model tested, when the compressor is turned off, the refrigerant fluid migrates to the evaporator, and the filter-dryer remains filled with vapor only. When the compressor is turned on the pressure at the filter-dryer rapidly increases and it can observed that the refrigerant vapor condenses. After some seconds, liquid flushes begin to reach the filter. Due to the stratification of the flow, the liquid accumulates at the bottom (Fig. 3, 4). While the liquid level is below the capillary tube tip, only vapor enters the capillary tube. With the progressive increase in the liquid level, at some point the liquid-vapor interface surpasses the capillary tube tip level, which starts to take in liquid.

From this moment onward, the amount of liquid refrigerant inside the filter-dryer is governed by the balance between the liquid mass flow rate coming from the condenser and the mass flow rate drained by the capillary tube. If the heat transfer rate at condenser is high, the liquid flow rate arriving at the filter-dryer is high and the liquid level rises, eventually filling up the filter-dryer. High heat transfer rate at condenser also enhances the degree of subcooling of the liquid, which allows for a higher mass flow rate through the capillary tube. When this overcomes the mass flow rate from the condenser, the liquid level at the filter-dryer lowers and the liquid-vapor interface approaches the capillary tube tip (Fig. 4a). Due to the acceleration of the liquid flow caused by suction into the capillary tube, a vortex is formed (Fig. 4b). The vortex flow allows vapor entrainment, that modifies the configuration of the flow through the capillary

tube, which becomes more restrictive due to the increase in the average speed of the flow and consequently in the rate of pressure drop by viscous dissipation.

(a) high liquid level (b) vortex formation (c) vortex intermittency

Figure 4. Flow condition at the capillary tube inlet (Test 8)

After the vortex inception, two conditions could be observed. If the flow rate arriving at the filter-dryer is higher, the reduction in the flow rate through the capillary tube due to vapor entrainment makes the liquid level rise again, interrupting the vortex formation (Fig. 4c). Consequently, the capillary tube takes in only liquid again, and the flow rate increases, lowering the liquid level, and the process restarts. Therefore, the flow stabilizes in an intermittent pattern, where the vortex is continuously created and interrupted, and the capillary tube takes in, alternately, liquid with vapor entrained or liquid only. However, when the flow rate from the condenser reduces, the intermittent behavior of the vortex does not occur. Instead, the vortex remains relatively stable (that is, it is not interrupted), with only slight oscillations in height, indicating that the flow rate through the capillary tube now equals that from the condenser.

The experimental observations confirmed the predicted behavior for this type of flow configuration (Takahashi *et al.*, 1988; Cristofano *et al.*, 2014). When the flow rate admitted by the capillary tube is high, inducing a high suction speed, the vortex can be formed when the liquid level is still high relative to the capillary tube tip, generating a long vortex (Fig. 5a), that is highly unstable and is continuously interrupted. If the suction speed is lower, the vortex will be generated when the liquid level is closer to the capillary tube tip (Fig. 5.b). This vortex is usually more stable.

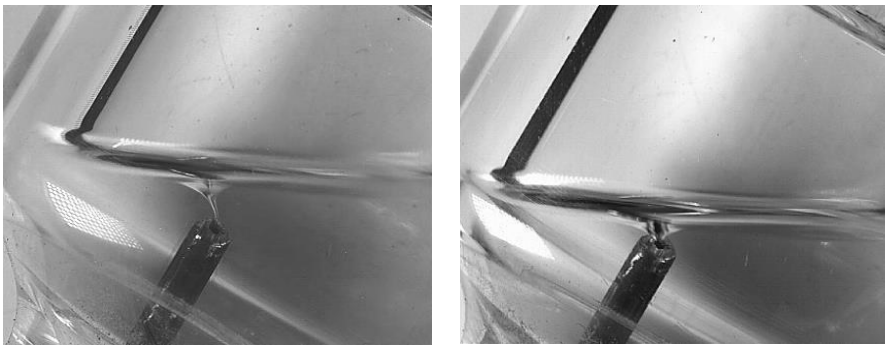

(a) long vortex (Test 4) (b) short vortex (Test 5)

Figure 5. Flow condition at the capillary tube inlet.

Table 4 summarizes the test conditions where the different types of vortex were observed. As expected, with the smaller-diameter capillary tube (0.520 mm), which yields higher restriction to the flow, the formation of the vortex was rarely observed, and the filter-dryer remained full of liquid during the operating cycle under almost all conditions. With larger diameters, once the vortex was formed, this condition remained until the end of the operating cycle. For the larger-diameter capillary tube (0.767 mm), which yields lower restriction, the continuous vortex regime prevailed, while for the intermediate diameter capillary tube (0.643 mm) the intermittent vortex regime was predominant.

When the rotational speed of the compressor is lowered, the flow stabilizes in the vortex formation regime (usually with a short continuous vortex) from the moment the liquid level reaches the capillary tube tip. Indeed, the rotational speed of the compressor has a strong effect on the condensing pressure and thus on the condenser heat transfer rate, that is, a lower compressor speed yields both a lower condensing pressure and lower condenser heat transfer rate, reducing the amount of liquid arriving at the filter-dryer.

Table 4. Tests with occurrence of vortex formation.

capillary tube ID [mm]	0.520	0.643	0.767
intermittent vortex	23, 34, 36	1, 2, 3, 4, 5, 8	9, 9D, 10, 10D, 25D
continuous vortex		7	11, 11D, 12, 12D, 13, 13D, 14, 14D, 15, 15D, 16, 16D, 25, 26, 26D, 27, 27D, 28, 28D, 29, 29D

3.2 Characterization of the operation of the refrigerating cycle

Figure 6 presents a comparison between a regular operating cycle and an after-defrost cycle, for the same operating condition. The highlight point on the curves indicates the moment of vortex formation. In a regular cycle, a rapid rise in the condensing pressure is observed (Fig. 6a) immediately after the compressor start-up, accompanied by a drop in the evaporating pressure (Fig. 6b).

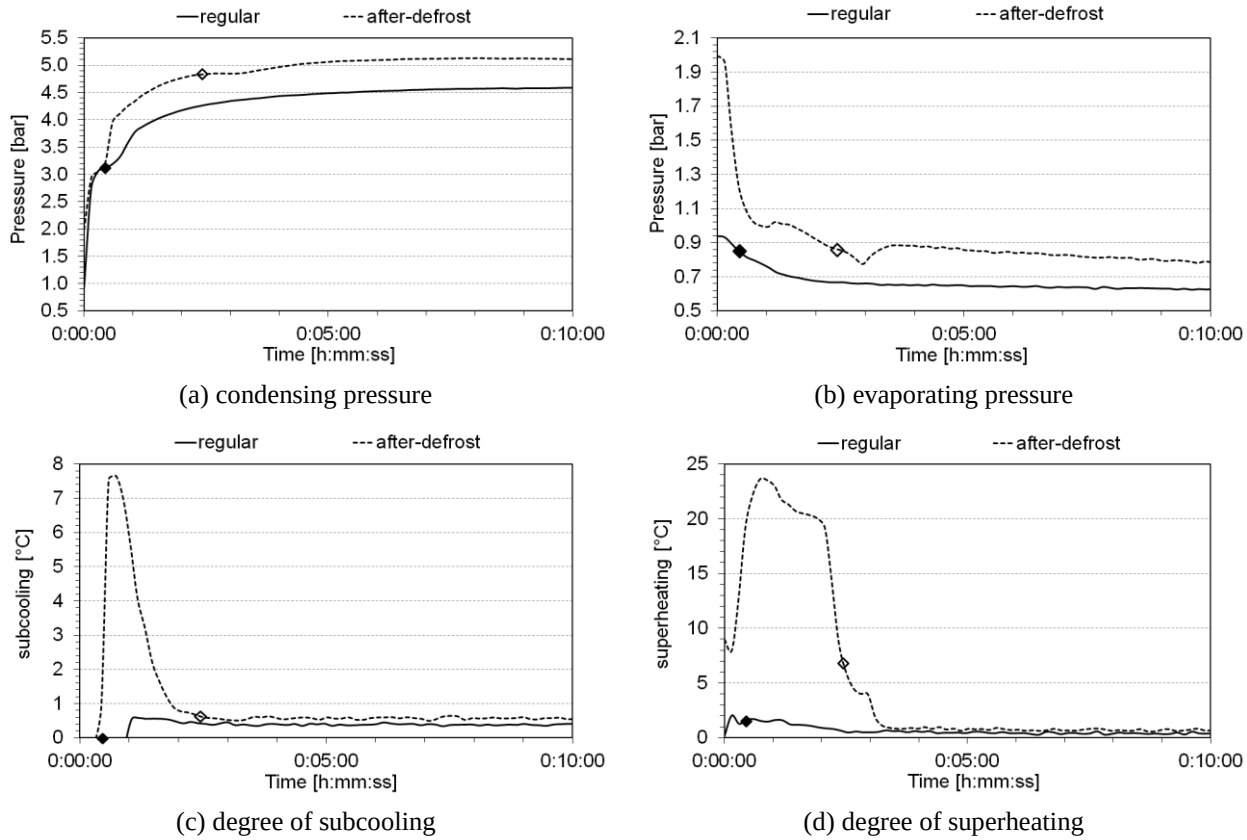

(a) condensing pressure

(b) evaporating pressure

(c) degree of subcooling

(d) degree of superheating

Figure 6. Comparison between regular and after-defrost cycle (Test 10)

It can be observed that the behavior of the pressures is greatly altered in the after-defrost cycle, especially in the first minutes of operation. During the defrost operation the heating of the evaporator causes vaporization of the liquid that is retained in it, and consequently the equalization pressure during the period when the compressor is off increases. Indeed, it can be observed from Fig. 6b that, while under normal conditions the equalization pressure of the system is approximately 0.92 bar, after the defrost operation this pressure reaches 2.0 bar. In this way, the rate of reduction of the evaporation pressure in the initial moments of the after-defrost cycle is much higher. It is noteworthy how pressures remain higher throughout the entire operating cycle.

The degree of subcooling (Fig. 6c) generally shows a small initial peak, but it quickly stabilizes, remaining fairly stable until the end of the cycle. When the visualization of the flow in the filter-dryer indicates the occurrence of vortex formation, the degree of subcooling is always low. In the condition depicted in Fig. 6, in the regular cycle, the vortex formation begins 27 s after the compressor start-up. In the after-defrost cycle, the degree of subcooling rises much more, reaching a peak shortly after the compressor start-up, and dropping rapidly thereafter, subsequently stabilizing at

approximately the same value observed in the regular cycle. This is reflected in the vortex formation time, which occurs only 2 min and 26 s after the compressor start-up.

In the regular cycle, the degree of superheating (Fig. 6d) typically rises during the initial moments when the thermal load on the evaporator is higher. As the temperature of the fresh-food and the freezer cabinet are reduced, the degree of superheating is also reduced. In the after-defrost cycle, it can be observed that the degree of superheating undergoes a much greater rise, as a consequence of the rapid reduction of the evaporating pressure and the high thermal load on the evaporator.

3.3 Characterization of the acoustic variables

This analysis is restricted to the acoustic pressure measured at the evaporator inlet, that is, after the capillary tube outlet, which showed greater relevance for the analysis of the expansion process (Boabaid Neto *et al.*, 2014; Tannert and Hesse, 2016).

During the operating cycle, this signal was found to be non-stationary, with a strong fluctuation of the global level. The typical spectral distribution (Boabaid Neto *et al.*, 2014) revealed that the intensity is inversely proportional to the frequency and no dominant tonal frequencies were observed. This spectral distribution is typical of subsonic jets (Lew *et al.*, 2010), that is, those generated by turbulent mixing. The increase in intensity level at higher frequencies, typical of shock-associated noise (Tam, 1995), was not observed, at least in the frequency range measured (10 Hz to 10 kHz). It was noted that the measured values for the Strouhal number were significantly lower than those generally observed for free aerodynamic jets and also lower than the results obtained by Reethof and Ward (1986) for confined compressed air jets. The power spectral density showed good agreement with the trends obtained by Lew *et al.* (2010) for subsonic jets.

Figure 7 shows typical results for the acoustic pressure during an entire operating cycle, for regular and after-defrost cycles, under the same operating condition. For better visualization, values for the acoustic pressure global level measurements are presented in decibel scale (referenced to the standard value of $2x10^{-5}$ Pa). For the regular cycle it can be observed that the global level remains almost constant. The fluctuation of the signal is notable.

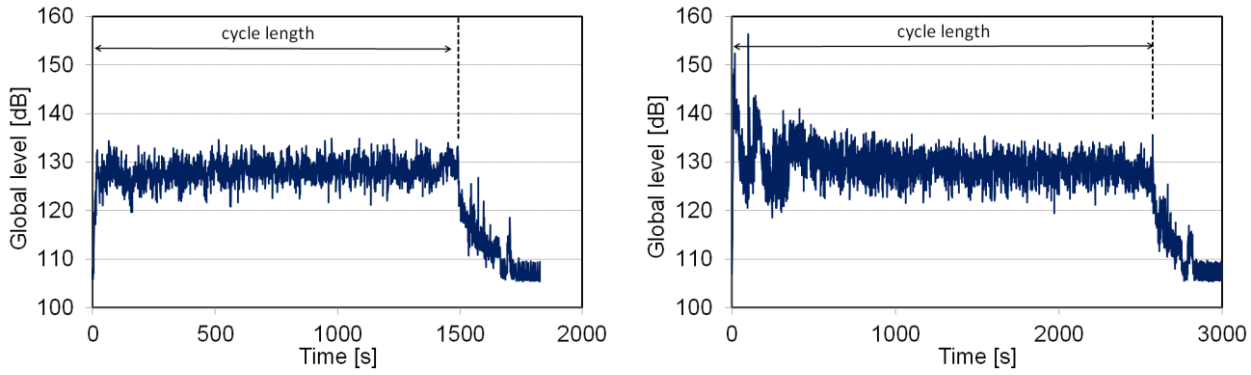

(a) regular cycle (b) after-defrost cycle

Figure 7. Level of acoustic pressure within the flow, evaporator inlet (Test 12).

In the after-defrost cycle (Fig. 7b), it was observed a strong increase of the acoustic pressure in the initial moments of the cycle, which is progressively reduced and tends towards stabilization. Indeed, as shown in the previous section, the operating conditions of the system were quite different in the initial moments of the after-defrost cycle, where it was observed that the rate of reduction of the evaporation pressure is much higher, along with a sharp increase in both the values of the subcooling at the capillary tube inlet and the superheating at the evaporator outlet. These conditions produce a higher mass flow through the capillary tube (as a consequence of the increase in the degree of subcooling), while the higher degree of superheating reduces the effectiveness of the heat exchanger, resulting in increased vaporization of the fluid along the capillary tube and greater vapor mass fraction at the outlet. Both effects result in higher average flow speed at the exit of the capillary tube. Thus, the after-defrost cycle is capable of generating greater mechanical power at the jet flow, resulting in greater acoustic energy generation (Singh *et al.*, 1999).

Figure 8 shows the evolution of the acoustic pressure for two different operating conditions, indicating the instant when the vortex formation begins. In the test condition of Fig. 8a, the liquid level in the filter-dryer initially increases, and the acoustic pressure level rises, accompanying the increase in the pressure ratio and in the degree of subcooling. The acoustic pressure level reaches a maximum value, then reduces and stabilizes, while the liquid level in the filter-dryer drops slowly. When the vortex formation begins, the increase in the fluctuation of the signal is noticeable, produced by an intermittent vortex formation pattern. In the condition of Fig. 8b, the increase of the liquid level in the

filter-dryer does not happen. When the liquid level reaches the tip of the capillary tube, the formation of a continuous vortex occurs, which remains quite stable, resulting in a much lower fluctuation of the signal.

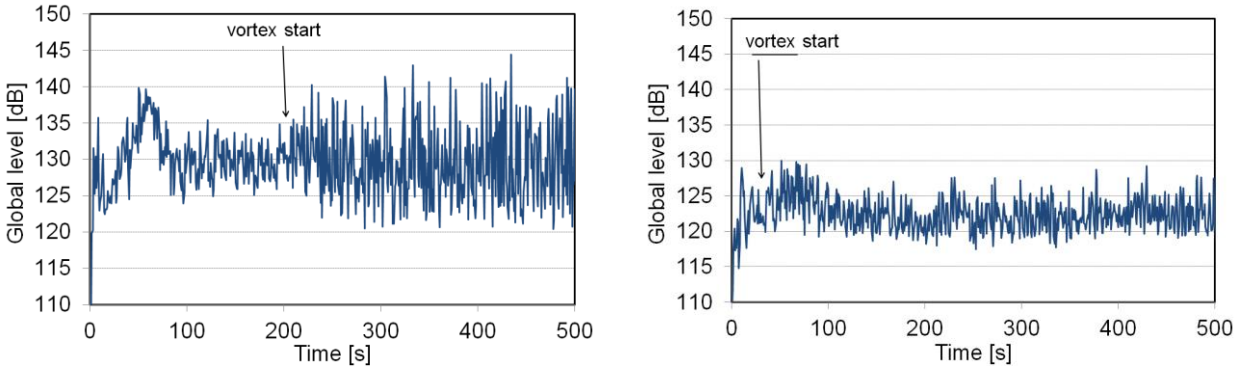

(a) Condition: Test 2 (b) Condition: Test 14

Figure 8. Level of acoustic pressure within the flow, evaporator inlet.

The fluctuation of the acoustic pressure is a consequence of the variation of the strength of the jet flow at the capillary tube outlet, which in turn is related to the discontinuous non-homogeneous two-phase flow patterns within the capillary tube. Revellin (2006) showed that for the flow of R134a refrigerant in tubes with inner diameters between 0.509 mm and 0.790 mm, the bubbly flow pattern (isolated bubbles) and the slug pattern predominate for values of vapor mass fraction of up to 15%, evolving to churn-like and annular patterns as the vapor mass fraction increases.

Apaydin and Heperkan (2016) undertook an experimental study where the two-phase flow patterns of the flow of refrigerant R-600a in a vertical adiabatic capillary tube of 0.80 mm inner diameter could be visualized. It was observed the occurrence of elongated vapor bubbles (that is, with an equivalent diameter greater than the inner diameter of the capillary tube, indicating a bubble/slug transition pattern), evolving to a slug pattern and to a annular pattern as the vapor mass fraction increases. The results showed a good agreement with the flow patterns observed by Revellin (2006), which confirms the occurrence of discontinuous non-homogeneous two-phase flow patterns for the R600a refrigerant flow inside capillary tubes.

Wang *et al.* (2017) investigated the relation between the flow pattern of R134a inside a transparent short tube (60 mm length and 1.4 mm ID) and the characteristics of the flashing jet spray at its outlet. They found that when the flow inside the tube is little disturbed, the jet morphology is very stable. But, when a slug two-phase flow pattern arrives at the nozzle outlet, the jet morphology was extremely unstable. Moreover, if it happens that a bubble of vapor enters the short tube, the flow is highly disturbed and so it is the jet.

Tannert and Hesse (2016) published an experimental study focusing on the flow in the capillary tube and its relation with the generation of noise in a refrigerator, which allowed the visualization of both the capillary tube inlet and outlet flow, as well as the two-phase flow pattern in the final section of the capillary tube. They observed that, when the capillary tube is taking in only liquid at its inlet, the flow at the capillary tube outlet consists of an undisturbed jet, and the two-phase flow pattern in the final section of the capillary tube was identified as annular. When the capillary tube inlet flow entrained vapor mixed with the liquid, the jet flow at the outlet becomes discontinuous, and a plug two-phase flow pattern in the final section of the tube is identified, with the occurrence of Taylor (elongated) bubbles. The authors measured the flow pressure after the capillary tube outlet and, in the first case descripted above, the pressure signal presented little oscillation; in the second case, the signal presented a significant amplitude change, which is accompanied by an increase in the level of acceleration and acoustic noise.

The results obtained in the present study were quite in agreement with the results obtained by Tannert and Hesse (2016) and others. It can then be concluded that the vortex formation amplifies the inherent fluctuation of the flow within the capillary tube due to the discontinuous two-phase flow patterns.

As showed by Takahashi *et al.* (1988), the vapor entrained at the vortex forms isolated bubbles as it enters the tube. When the flow reaches the region of the heat exchanger and the flow is cooled, the fluid will be recondensed, which causes the isolated bubbles to oscillate, increasing the oscillation in the flow. In the case of the intermittent vortex pattern, in which the vortex is continuously created and destroyed, the flow in the initial section of the capillary tube is continuously alternated between a pattern of isolated bubbles and a purely liquid flow, further increasing the disturbance on the flow. So, the intermittent vortex pattern yields a larger amplitude of the acoustic pressure fluctuation than for the continuous vortex pattern.

As stated, averages of all measurements were taken from samples of the signals extracted at 2-min intervals during the period of greatest stabilization of the cycle. In the case of acoustic pressure, the standard deviation values of these averages are a good indicator of the magnitude of the fluctuation of the signal. This average was 12.5, 18.7 and 9.1 Pa, respectively for the no-vortex (NV), intermittent (VI) and continuous (VC) vortex conditions. The intermittent vortex

condition yielded the greater value, as expected. But unexpectedly the value for the continuous vortex was the lowest. This can be explained by the fact that there is a direct correlation between the mean value and the standard deviation value, and for the VC condition the acoustic pressure values were lower on average than for the NV condition (see Fig. 10). Moreover, as in the NV condition the fluid at the capillary tube inlet is liquid and showed on average a higher degree of subcooling, it is expected the vapor mass fraction at the capillary tube outlet to be lower, increasing the probability that the two-phase flow pattern is of the slug type, while in the VC condition, as stated, vapor already exists from the capillary tube inlet and consequently the vapor mass fraction at the capillary tube outlet is larger, leading to the predominance of annular two-phase flow pattern.

Acceleration measurements at the tube walls showed to be very sensitive to structural modifications in the refrigerator, and so significant changes were observed after any disassembly and reassembly procedure (required to mount the instrumentation, for example) to which the refrigerator was subjected. Thus, it was not possible to establish a consistent and reliable quantitative relationship between the excitation in the flow and the structural excitation. Despite this, the acceleration measurements were able to qualitatively reproduce most of the effects observed in the acoustic pressure measurement, and a direct relationship between the two quantities could be inferred.

The hearing of the audible signal from the accelerometer installed at the evaporator inlet showed that, during the stabilized operation period (with intermittent or continuous vortex) the signal qualitatively resembles a whistling noise, whose tone varies with the intermittence of the vortex. In the condition of continuous vortex, there is less variation of the tone. When there is no vortex formation, qualitatively the signal resembles that of the continuous vortex condition, reinforcing the conclusion that the flow pattern inside the capillary tube induces an oscillation of the jet flow. In general, the ambient noise generated by the expansion process was practically imperceptible.

3.4 Factorial analysis

For the factorial analysis the set of 24 tests in normal operating conditions, that is, those indicated in Table 2, were used. Figure 9 shows the individual effect of each factor on the acoustic pressure at evaporator inlet, where p' denotes the global level (*rms* value). Errors bars show the confidence interval for 95% probability.

The effect of the inner diameter of the capillary tube is presented in Fig. 9a. With the increase of the inner diameter there is a slight increase in the condensing pressure but a stronger increase in the evaporating pressure. There is a reduction of the degree of superheating, and for the two largest diameters the degree of subcooling is very small, a consequence of the fact that, for these cases, the vortex formation condition prevailed. Despite the expected large increase in mass flow rate through the capillary tube, the acoustic pressure is reduced.

From Fig. 9b it can be observed that the refrigerant charge was the factor of greater effect. The increase in the charge resulted in a slight increase in both the evaporating and the condensing pressures, resulting however in a slight reduction of the pressure ratio across the capillary tube. The degree of superheating is also reduced, whereas the degree of subcooling is practically unaffected. Thus, there is little influence of the charge on the mass flow and the vapor mass fraction at the capillary tube outlet. However, the increase in refrigerant charge favored the occurrence of continuous vortex condition.

When the compressor speed increases (Fig. 9c), it is observed the reduction of the evaporating pressure and increase of the condensing pressure, resulting in a significant increase of the pressure ratio across the capillary tube. There is also an increase in both the degrees of subcooling and superheating, however the evaporator outlet temperature is reduced. These effects combined yield an increase in the mass flow and a reduction in the vapor mass fraction at the capillary tube outlet.

The increase in ambient temperature resulted in a significant increase of the condensing pressure, and a smaller increase in the evaporating pressure, resulting in an increase in the pressure ratio, while the degrees of subcooling and superheating were little affected. As a result, an increase in the mass flow rate and in the vapor mass fraction is to be expected. Nevertheless, the increase in ambient temperature resulted in a small reduction of the acoustic excitation, as shown in Fig. 9d.

The vortex formation phenomenon proved to be a significant factor in the performance of the refrigeration system, although it was not a controlled factor of the experiment, but a consequence of the others. For the larger diameter capillary tube the continuous vortex prevailed whereas for the smaller diameter capillary tube the vortex formation was practically eliminated. For the intermediate capillary tube diameter, the intermittent vortex condition prevailed (Table 4). When the vortex formation occurred the degree of subcooling was quite low whereas for the condition without vortex the values were much higher. Conditions that yielded the vortex formation also showed a reduced degree of superheating, higher evaporating pressure, lower expansion ratio through the capillary tube, and higher temperature difference between the capillary tube inlet and the evaporator outlet. In Fig. 10 it can be observed that there is no statistically significant difference between the values of the acoustic pressure for the intermittent vortex condition (VI) and the condition without vortex formation (NV), but the continuous vortex condition (VC) presented significantly lower values.

As explained, the refrigeration system shows a different behavior in the after-defrost cycle, especially during the first minutes of operation. Figure 11 shows the comparison between the mean values of acoustic pressure for regular

cycles and for the after-defrost cycles. It is evident that the after-defrost cycle provides more favorable conditions to the generation of acoustic excitation throughout the entire cycle of operation, even when the cycle is in its period of stabilized operation. This behavior is corroborated by the analysis of Fig. 7.

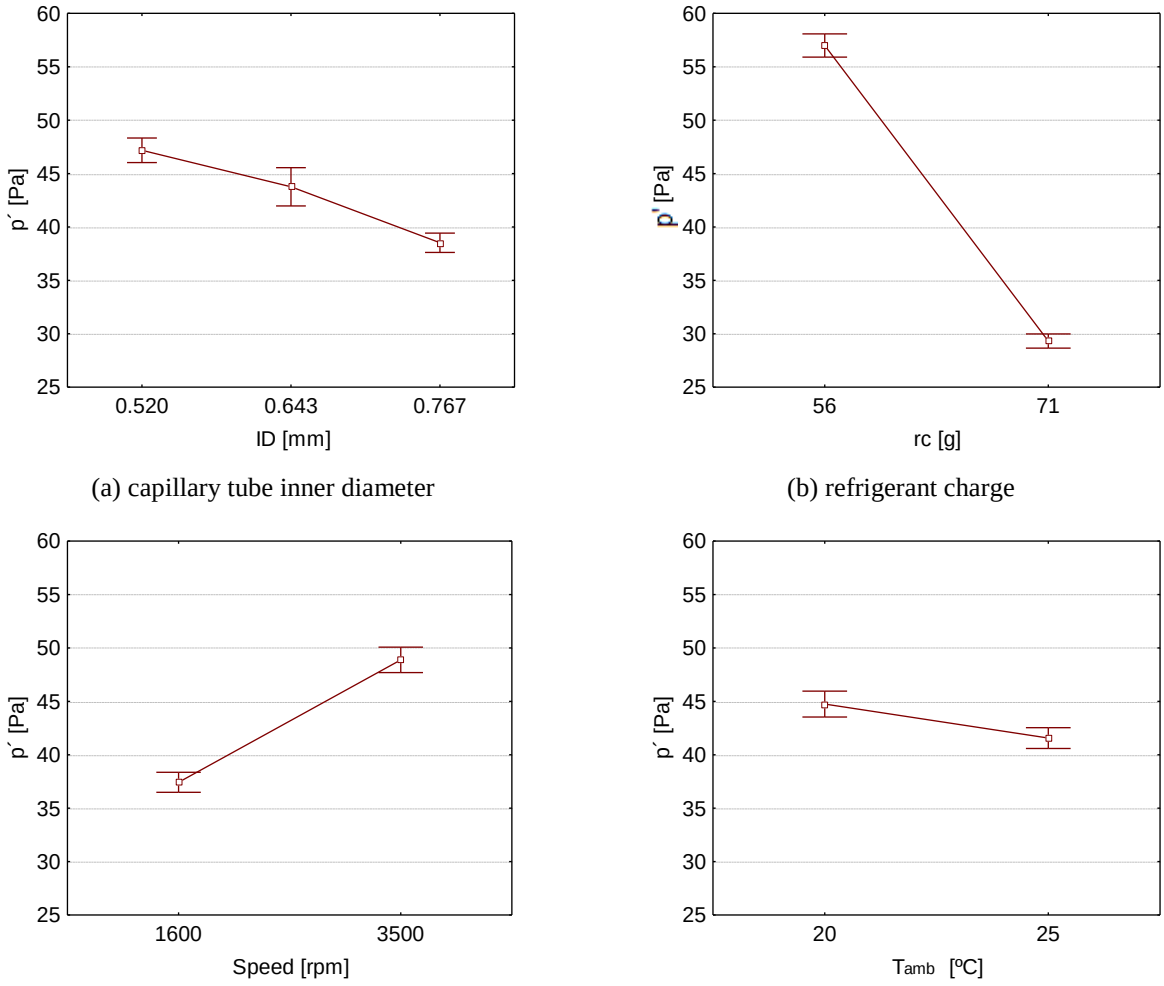

(a) capillary tube inner diameter

(b) refrigerant charge

(c) compressor rotational speed

(d) ambient temperature

Figure 9. Effect of the factors of the experimental design

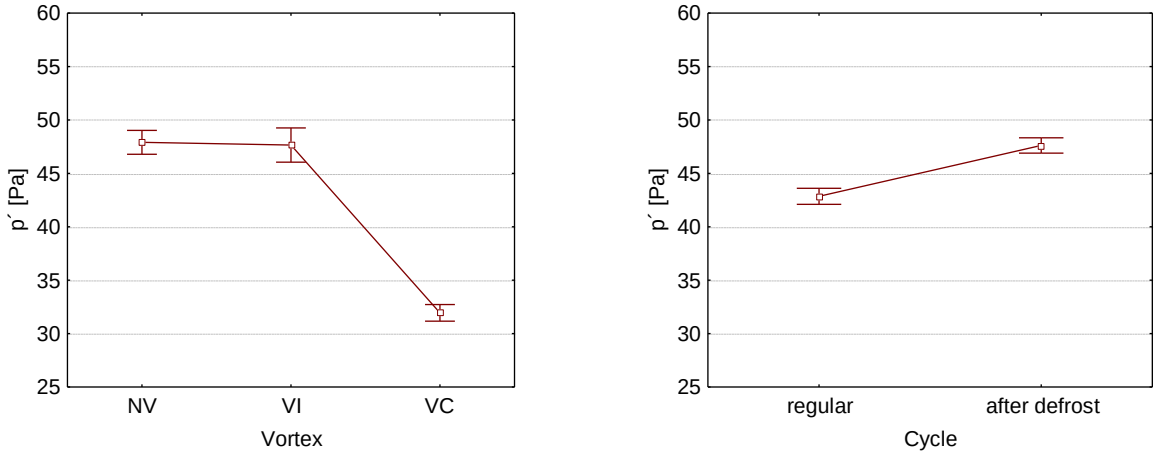

Figure 10. Effect of the vortex formation pattern

Figure 11. Effect of the type of cycle

The results demonstrated a complex interaction between all the physical quantities. The understanding of the effect of the factors on the acoustic pressure depends on the knowledge of the physical processes of acoustic generation by the jet flow and its relation to the characteristics of the flow through the capillary tube. These aspects will be addressed in future work.

4. CONCLUSIONS

An experimental study focused on the expansion noise in a household refrigerator equipped with capillary tube has been presented. The study innovatively employed the direct measurement of the acoustic pressure within the refrigerant flow. By visualizing the flow at the filter-dryer, it has been found that over a wide range of operating conditions a vortex is formed at the capillary tube inlet, which allows it to entrain refrigerant vapor. The vortex formation generates oscillations in the flow, especially with the intermittent vortex pattern as it continuously changes the distribution of the vapor along the capillary tube.

The study confirmed that the jet flow at the capillary tube outlet is the dominant mechanism for the generation of acoustic excitation associated to the expansion process. The acoustic pressure signal has the characteristic of a turbulent mixing excitation, typical of a subsonic jet. The global level of the acoustic pressure shows an oscillating behavior, that is primarily related to the oscillation of the flow due to the discontinuous two-phase flow patterns occurring in the capillary tube. When the vortex is formed, the amplitude of oscillation is increased.

The acoustic excitation global levels showed the lowest values in the conditions that allowed the formation of a continuous vortex. Results also showed that a larger diameter capillary tube produced lower levels of acoustic excitation, because it enables the continuous vortex pattern, especially when combined with a higher refrigerant charge.

Reducing the speed of the compressor had the effect of reducing the acoustic excitation, while the reduction of the ambient temperature increased the acoustic excitation. The initial period of the operating cycle of the system was the most critical, due to the rapid and intense variation in the operating conditions. Finally, acoustic pressure showed to be higher in after-defrost cycles.

The experimental results clearly indicate that the combination of a larger capillary tube inner diameter with higher refrigerant charge would be a solution for reducing the acoustic pressure. However, as demonstrated by Boeng and Melo (2012), the simultaneous increase of the inner diameter and the refrigerant charge has the effect of increasing the consumption of the refrigerator.

As the defrost procedure showed to be particularly critical for acoustic excitation, modifications in this procedure that could reduce evaporator heating and equalization pressure would have the potential to reduce the acoustic excitation generated in the first operating cycle after defrost.

The results suggest that the use of lower compressor speed during the first minutes of operation of the refrigeration cycle has the potential to reduce the acoustic excitation. Compressor speed should be progressively increased in small increments so as not to generate sudden gradients in the flow variables.

The importance of the acoustic excitation generated by the jet flow at the capillary tube outlet suggests a modification of the geometry of the transition between the capillary tube and the evaporator inlet, in order to dissipate the mechanical and acoustic energy of the jet stream. As the acoustic excitation is primarily caused by the turbulent eddies formed at the jet interface (Lighthill, 1963), it can be concluded that the presence of some kind of structure placed immediately after the capillary tube outlet that could change the jet configuration and affect the formation of the eddies would be the most effective measure for reduction of the acoustic excitation generated by the jet under any operating conditions, possibly eliminating the need for further modifications that could alter the energy performance of the system. Indeed, Singh *et al.* (1999) showed that metallic screens positioned at an orifice tube outlet significantly reduced sound pressure levels under all operating conditions.

It is noteworthy that the study clearly demonstrated that the transmission of vibratory energy through the structure of a refrigerator is in fact the dominant mechanism in the process of generating audible noise from the refrigerant flow. Therefore, in order to evolve the understanding and control of the noise in this kind of equipment, it is necessary to deepen the study of the transmission paths of vibratory energy through a complex structure such as a refrigerator.

5. ACKNOWLEDGEMENTS

This study was made possible through the financial support from the EMPRAPII Program (POLO-UFSC-EMPRAPII Unit – Emerging Technologies in Cooling and Thermophysics). The authors are grateful to Messrs. R. Freitas, R. Góes, M. Seifert, J. Lubas, D. Oliveira, K. Rosa, G. Pianovski, J. Tenfen, A. Lessa, and Miss N. Sá, for their help and technical support. Financial support from Whirlpool Latin America S. A. is also acknowledged.

6. REFERENCES

ASHRAE, 1996. *ANSI/ASHRAE Standard 28-1996, Method of testing flow capacity of refrigerant capillary tubes.* Atlanta, GA: American Society of Heating, Refrigeration and Air Conditioning Engineers Inc.

Apaydin, T., and Heperkan, H., 2016. "Experimental investigation of R600a refrigerant flow inside adiabatic capillary tube". *Sigma J Eng & Nat Sci*, Vol. 34(2), p. 241-252.

Boabaid Neto, C., Melo, C., Lenzi, A., and Caetano, A.L.G., 2014. "Noise generation in household refrigerators: an experimental study on fluid-borne noise". In *Proceedings of the 15th International Refrigeration and Air Conditioning Conference*. West Lafayette, USA. <http://docs.lib.purdue.edu/iracc/1371>.

Boeng, J., Melo, C., 2012. "A capillary tube-refrigerant charge design methodology for household refrigerators – Part II: equivalent diameter and test procedure". In *Proceedings of the 14th International Refrigeration and Air Conditioning Conference*. West Lafayette, USA. <http://docs.lib.purdue.edu/iracc/1180>.

Box, G.E.P., Hunter , J.S., and Hunter, W.G., 2005. *Statistics for Experimenters*. John Wiley & Sons, Hoboken, NJ, 2nd edition.

Caetano, A.L.G., 2013. *Study of the noise generated by gas expansion in the evaporator of a household refrigerator*. M.Eng. thesis, Federal University of Santa Catarina, Florianópolis, SC, Brazil.

Chen, D.K., 1997. *Flashing flow of refrigerant HFC-134a through a diabatic capillary tube*. Ph.D. thesis, Department of Mechanical Engineering, Concordia University, Montreal, CA.

Cristofano, L., Nobili, M., and Caruso, G., 2014. "Experimental study on unstable free surface vortices and gas entrainment onset conditions". *Exp. Therm. Fluid Sci.*, Vol. 52, p. 221-229.

Hartmann, D., and Melo, C., 2013. "Popping noise in household refrigerators: fundamentals and practical solutions". *Appl. Therm. Eng.*, Vol. 51, p. 40-47.

JCGM, 2008. JCGM 100:2008: Evaluation of measurement data - Guide to the expression of uncertainty in measurement. <http://www.bipm.org/utils/common/documents/jcgm/JCGM_100_2008_E.pdf>.

Jeon, J. Y., You, J., Chang, H. Y., 2007. "Sound radiation and sound quality characteristics of refrigerator noise in real living environments". *Appl Acoust*, Vol. 68, p. 1118-1134.

Lew, P.T., Mongeau, L., and Lyrintizis, A., 2010. "Noise prediction of a subsonic turbulent round jet using the lattice-Boltzmann method". *J. Acoust. Soc. Am.*, Vol. 128(3), p. 1118-1127.

Lighthill, M.J., 1963. "Jet noise". *AIAA Journal*, Vol. 1(7), p. 1507-1517.

McGee, R., 2009. "Auditory displays and sonification: introduction and overview". The University of California, Santa Barbara. <http://www.lifeorange.com/writing/Sonification_Auditory_Display>.

McLevige, S.M., and Miller, N.R., 2001. *Experimental investigation of the source of acoustic bursts produced by household refrigerators*. Technical report TR-184. Air Conditioning and Refrigeration Center, University of Illinois, Urbana. <http://citeseerx.ist.psu.edu/viewdoc/download?doi=10.1.1.261.1414&rep=rep1&type=pdf>.

Möller, G., Detert, M., and Boes, R.M., 2012. "Air entrainment due to vortices - state-of-the-art". In *Proceedings of the 2nd IAHR Europe Congress*. Paper B16. Munich, Germany.

Reethof, G., 1978. "Turbulence-generated noise in pipe flow". *Ann. Rev. Fluid Mech.*, Vol. 10, p. 333-367.

Reethof, G., and Ward, W.C., 1986. "A theoretically based valve noise prediction method for compressible fluids". *J. Vib., Acoust., Stress, and Reliab*, Vol. 108(3), p. 329-338.

Revellin, R., 2006. *Experimental two-phase flow in microchannels*. Thèse Docteur ès sciences, Faculté Sciences et Techniques de l´Ingénieur, Institut des Sciences de l´Énergie, Section de Génie Mécanique, École Polytechnique Fédérale de Lausanne, Lausanne. <https://infoscience.epfl.ch/record/62762/files/EPFL_TH3437>.

Singh, G.M., Rodarte, E., Miller, N.R., and Hrnjak, P.S., 1999. *Noise generation from expansion devices in refrigerant*. Technical Report TR-152. Air Conditioning and Refrigeration Center, University of Illinois, Urbana, IL. <http://citeseerx.ist.psu.edu/viewdoc/download?doi=10.1.1.553.8595&rep=rep1&type=pdf>.

Takahashi, M., Inoue, A., Aritomi, M., Tanekaka, Y., and Suzuki, K., 1988. "Gas entrainment at free surface of liquid (II). Onset conditions of vortex-induced entrainment". *J. Nucl. Sci. Technol.*, Vol. 25(3), p. 245-253.

Tam, C.K.W., 1995. "Supersonic jet noise". *Ann. Rev. Fluid Mech.*, Vol. 27, p. 17-43.

Tannert, T., and Hesse, U., 2016. "Noise effects in capillary tubes caused by refrigerant flow". In *Proceeding of the 16th International Refrigeration and Air Conditioning Conference at Purdue*. West Lafayette, USA. <https://docs.lib.purdue.edu/iracc/1562/>.

Wang, X. S., Chen, B., Wang, R., Xin, H., Zhou, Z. F., 2017. "Experimental study on the relation between internal flow and flashing spray characteristics of R134a using straight tube nozzles". *Int. J. Heat Mass Transf.*, Vol. 115, p. 524-536.

Wallis, G. B., 1980. "Critical two-phase flow". *Int J Multiphas Flow*, Vol. 6, p. 97-112.

7. RESPONSIBILITY NOTICE

The authors are the only responsible for the printed material included in this paper.